MATHEMATICAL BIOSCIENCES
AND ENGINEERING
Volume **9**, Number **3**, July **2012**

doi:10.3934/mbe.2012.9.647

pp. **647–662**

A MATHEMATICAL MODEL FOR WITHIN-HOST *TOXOPLASMA GONDII* INVASION DYNAMICS

Adam Sullivan

Department of Mechanical, Aerospace, and Biomedical Engineering
University of Tennessee, Knoxville, TN 37996, USA

Folashade Agusto

Department of Mathematics and Statistics
Austin Peay State University, Clarksville, TN 37044, USA

Sharon Bewick

National Institute of Mathematical and Biological Synthesis
University of Tennessee, Knoxville, TN 37996, USA

Chunlei Su

Department of Microbiology
University of Tennessee, Knoxville, TN 37996, USA

Suzanne Lenhart

Department of Mathematics
University of Tennessee, Knoxville, TN 37996, USA

Xiaopeng Zhao*

Department of Mechanical, Aerospace, and Biomedical Engineering
University of Tennessee, Knoxville, TN 37996, USA

(Communicated by Jia Li)

Abstract. Toxoplasma *gondii* (T. *gondii*) is a protozoan parasite that infects a wide range of intermediate hosts, including all mammals and birds. Up to 20% of the human population in the US and 30% in the world are chronically infected. This paper presents a mathematical model to describe intra-host dynamics of *T. gondii* infection. The model considers the invasion process, egress kinetics, interconversion between fast-replicating tachyzoite stage and slowly replicating bradyzoite stage, as well as the host's immune response. Analytical and numerical studies of the model can help to understand the influences of various parameters to the transient and steady-state dynamics of the disease infection.

1. **Introduction.** *Toxoplasma gondii*, often referred to as *T. gondii*, is a parasite that is able to infect a wide range of hosts, including all mammals and birds [13]. Up to one third of the world's human population and about 20% of the population in the US are estimated to carry a Toxoplasma infection [1]. People can be infected by eating infected meat, by drinking water contaminated with the parasite, or by transmission from mother to fetus. During acute Toxoplasma infection, the patient

2000 *Mathematics Subject Classification.* Primary: 37N25, 92B05; Secondary: 93A30.

Key words and phrases. Toxoplasma gondii, stage conversion, parasite infection, within-host invasion, intra-host dynamics.

∗ Corresponding author.

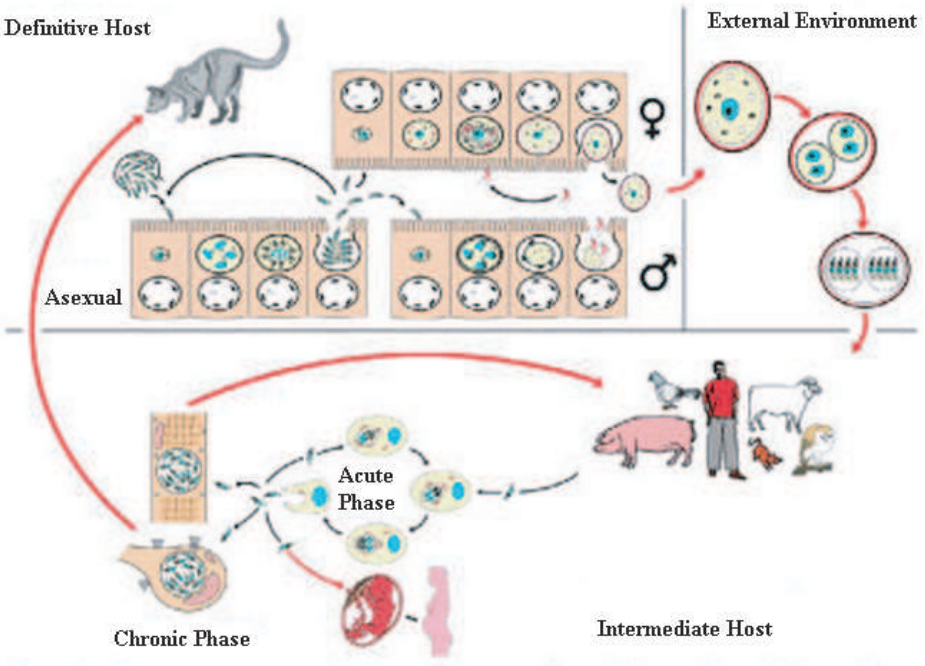

FIGURE 1. Diagram representing the life cycle of *T. gondii*. Reprinted from [15] with permission from Elsevier.

typically exhibits a mild flu-like illness (swollen lymph nodes, or muscle aches and pains that last for a month or more) or no illness at all. However, people with a weakened immune system, such as AIDS patients or recipients of chemotherapy and organ transplant, may develop serious inflammation in the brain or the eyes. In most immunocompetent patients, the infection enters a latent phase, during which tissue cysts may form in the brain and muscle. Recent studies show that latent Toxoplasmosis may have significant effects on human behavior and may lead to neuropsychiatric disorders, e.g. schizophrenia. In addition, infection acquired during pregnancy may spread and cause severe damage to the fetus [1].

T. gondii has a complex life cycle, as seen in Figure 1. The parasite uses the feline to reproduce sexually. When the cat becomes infected, it sheds oocysts, which infect the environment. These oocysts can be ingested by mammals and birds which then become infected with the parasite [13]. Eating another organism that is infected can also infect the secondary hosts. A few mathematical models have been developed to investigate the transmission dynamics of *T. gondii* between different hosts [5, 19, 24, 25, 38].

Within a host, *T. gondii* exists in two interconvertable stages: bradyzoites and tachyzoites. Bradyzoites have the slow-growing and encysted form whereas tachyzoites are the fast-replicating parasites. Tachyzoites disseminate within the host and lead to the acute phase of infection. After the bradyzoite-containing cysts are ingested by the host, the walls of these cysts are digested inside the host's stomach. Bradyzoites, which are resistant to gastric conditions in the stomach, will subsequently invade the host's epithelial cells of the small intestine and convert into

tachyzoites there. While most of tachyzoites in immunocompetent hosts are eliminated by the innate and adaptive immune responses, some tachyzoites differentiate into the dormant bradyzoite stage inside host cells [13]. The differentiation of tachyzoites into the bradyzoite stage plays an essential role in the development of tissue cysts, which allows life-long persistence of the parasites in the host. Reactivation of bradyzoites back to tachyzoites can lead to life threatening infection. The interconversion between tachyzoites and bradyzoites can be influenced by many in vivo and in vitro factors. In this work, we aim to develop a mathematical model to understand the nonlinear, complex interactions between *T. gondii* invasion dynamics and host immune response.

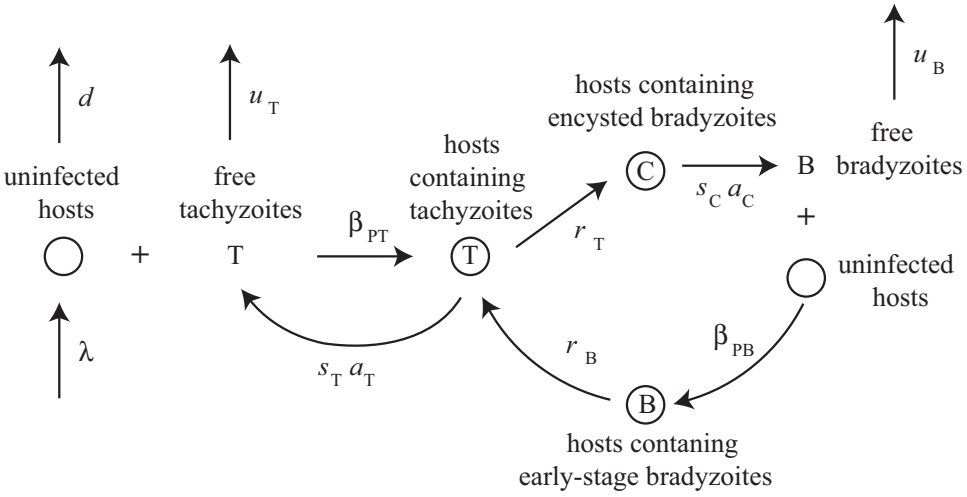

FIGURE 2. Compartmental model representing within-host invasion dynamics of *T. gondii*. Note the immune response is not shown.

2. **Model development.** We develop a compartmental model to describe the invasion dynamics of *T. gondii*; see Figure 2. The model has 7 state variables: the population size of uninfected cells, X; the population of cells infected with tachyzoites, Y_T; the population of cells containing early-stage bradyzoites, Y_B; the population of cells containing encysted bradyzoites, Y_C; the population of free tachyzoites, P_T; the population of free bradyzoites, P_B; and the effector cells of the host's immune response, Z.

We assume uninfected cells are generated at a constant rate of λ and assume the average life time of an uninfected cell is $1/d$. In the absence of an infection, the population dynamics of host cells is given by $\dot{X} = \lambda - dX$. Under this simple population dynamics model, the number of uninfected cells converges to the equilibrium $X_0 = \lambda/d$. Free parasites infect uninfected cells at a rate proportional to the product of their abundance: $\beta_{PT} X P_T$ for tachyzoites and $\beta_{PB} X P_B$ for bradyzoites. The rate constants, β_{PT} and β_{PB} describe the efficacy of the invasion process and depend on the rate at which the parasites find uninfected cells, the rate of parasite entry, and the probability of successful infection. Note that β_{PT} and β_{PB} are lumped parameters and have the unit 1/(number of cells)/time [27, 30, 31, 41].

Note these rate constants sometimes carry a slightly different definition; see [6] for example.

Average life time of a cell infected with tachyzoites is $1/a_T$ and that of a cell infected with encysted bradyzoites is $1/a_C$. Since tachyzoites replicate much faster than bradyzoites, one expect a_C be much smaller than a_T. Assume the total number of parasites produced from one infected cell containing tachyzoites, i.e. the burst size, is s_T and assume the burst size of an encysted cell is s_C. Let $k_T = s_T * a_T$ and $k_C = s_C * a_C$. Then, free parasites are produce at a rate $k_T y_T$ for tachyzoites and $k_C y_C$ for encysted bradyzoites. Free parasites are removed from the system at a rate $u_T P_T$ for tachyzoites and at rate $u_B P_B$ for bradyzoites. Tachyzoites in a host cell can spontaneously convert to bradyzoites at a rate $r_T y_T$. To account for the reactivation process, we assume early-stage bradyzoites may convert to tachyzoites at a rate $r_B y_B$. We also consider a simple model for the immune response. Much work has been done regarding the immune response caused by Toxoplasma infection and many important mechanisms have been identified [16]. Here, we introduce a variable Z to represent the overall effector cells without consideration of specific immune mechanisms. We assume the effector cells act on host cells infected with tachyzoites in a predator-prey manner.

Combining the above processes leads to the following system of equations:

$$\dot{X} = d(X_0 - X) - \beta_{PT} X P_T - \beta_{PB} X P_B \tag{1}$$

$$\dot{Y}_T = \beta_{PT} X P_T - a_T Y_T - r_T Y_T + r_B Y_B - c_T Y_T Z \tag{2}$$

$$\dot{Y}_C = r_T Y_T - a_C Y_C \tag{3}$$

$$\dot{Y}_B = \beta_{PB} X P_B - r_B Y_B \tag{4}$$

$$\dot{P}_T = k_T Y_T - u_T P_T \tag{5}$$

$$\dot{P}_B = k_C Y_C - u_B P_B \tag{6}$$

$$\dot{Z} = \frac{\rho Y_T Z}{h + Y_T} - \delta Z \tag{7}$$

where ρ is the production rate of the effector cells, δ is the removal rate of the immune system response, and h represents the saturation level of the effector cells [41]. The first term in the immune equation represents the activation process in response to the detection of infected cells whereas the second term in the immune equation represents natural decay of the immune effector. The activation process takes the form of Holling's Type II predator-prey relation [28, 36, 8]. When the number of infected cells is small, the level of immune response is low. Then, the immune response increases at a great rate and saturates when the number of parasites is sufficiently large.

Kafsack *et al.* [26] developed a mathematical model to interpret kinetics data collected for T. gondii invasion. Their results show that T. gondii invasion dynamics including contact, attaching, penetrating, and invasion occur within a few minutes. On the other hand, previous experiments show that replication and stage conversion dynamics take place in hours [23, 13, 40]. We assume that the kinetics of free parasites are significantly faster than kinetics of other processes. Thus, we can adopt the common quasistationary approximation and assume the free parasites

are in equilibrium. It follows from Equations (5)-(6) that

$$P_T = \frac{k_T Y_T}{u_T} \tag{8}$$

$$P_B = \frac{k_C Y_C}{u_B} \tag{9}$$

Substituting the above equations into Equations (1)-(4), (7) leads to the following reduced model:

$$\dot{X} = d(X_0 - X) - \beta_T Y_T X - \beta_B Y_C X \tag{10}$$

$$\dot{Y}_T = \beta_T Y_T X - a_T Y_T - r_T Y_T + r_B Y_B - c_T Y_T Z \tag{11}$$

$$\dot{Y}_C = r_T Y_T - a_C Y_C \tag{12}$$

$$\dot{Y}_B = \beta_B Y_C X - r_B Y_B \tag{13}$$

$$\dot{Z} = \frac{\rho Y_T Z}{h + Y_T} - \delta Z, \tag{14}$$

where $\beta_T = k_T \beta_{PT}/u_T$ and $\beta_B = k_C \beta_{PB}/u_B$. A compartmental model of this simplified model is shown in Figure 3. All parameters in the model are non-negative and one can show that the solutions of the system are non-negative, given non-negative initial values. The model (10)-(14) will be analyzed in a biologically-feasible region as follows. We consider the region

$$\mathcal{D} = \left\{(X, Y_T, Y_C, Y_B, Z) \in \mathbb{R}^5_+ : X \geq 0, Y_T \geq 0, Y_C \geq 0, Y_B \geq 0, Z \geq 0\right\}.$$

Solutions of (10)-(14) starting in $\mathcal{D}$ can be shown to remain in $\mathcal{D}$ for all $t \geq 0$. Thus $\mathcal{D}$ is positively invariant and it is sufficient to consider solutions in $\mathcal{D}$. We state and prove Theorem 2.1 for non-negativity of solutions of (10)-(14) in $\mathcal{D}$.

Theorem 2.1. *Let the initial data be $X(0) \geq 0$, $Y_T(0) \geq 0, Y_C(0) \geq 0, Y_B(0) \geq 0$, and $Z(0) \geq 0$. Then, solutions $X(t)$, $Y_T(t)$, $Y_C(t)$, $Y_B(t)$ and $Z(t)$ of the model system (10)-(14) are non-negative for all $t \geq 0$. Moreover, for the model system (10)-(14), the region $\mathcal{D}$ is positively invariant.*

Proof. Assume that the solution of (10)-(14) has been extended to maximal domain $[0, T^*)$; we will show the non-negativity of solutions and that there is no blow-up, giving $T^* = \infty$.

Since $X_0 > 0$ and the other terms in the right hand side (RHS) of equation (10) has X as a common factor, we have that $X(t) \geq 0$ for $t \geq 0$. Similarly, the structure of the RHS of (14) implies that $Z(t) \geq 0$ for $t \geq 0$.

Note that the structure of (11)-(13) implies that if $Y_T(0) = Y_C(0) = Y_B(0) = 0$, then $Y_T(t) = Y_C(t) = Y_B(t) = 0$ for all $0 \leq t \leq T^*$ by uniqueness of the initial boundary value problem (solution is $(X(t), 0, 0, 0, Z_0 e^{-\delta t})$ where $X' = d(X_0 - X)$).

If one of $Y_T(0), Y_C(0)$ or $Y_B(0)$ is positive, then we can show that all three components are positive on $[0, T^*)$. For example if $Y_C(t) > 0$ on $[0, \epsilon]$, by integrating the DEs for Y_B and Y_T, we obtain their positivity on $[0, \epsilon]$. On the other hand, if one of these three functions hits 0, say Y_T, let t_1 be the first time that Y_T is 0 and all three functions are positive on $(0, t_1)$. The structure of (11) with $K(t) = \beta_T X(t) - a_T - r_T - c_T Z(t)$ gives

$$Y_T(t_1) e^{\int_0^{t_1} K(s)ds} - Y_T(0) = \int_0^{t_1} e^{\int_0^t K(s)ds} r_B Y_B(t) dt,$$

which is a contradiction as the RHS is positive, $Y_T(t_1) = 0$ and $Y_T(0) \geq 0$. Continuing we conclude that D is invariant.

The structure of (10) and (14) shows that X and Z do not blow up. Note that

$$M(t) = X(t) + Y_T(t) + Y_C(t) + Y_B(t)$$

satisfies

$$M'(t) \leq d(X_0 - X(t)),$$

which means that M does not blow up. Thus we conclude $T^* = \infty$. □

Note that for $\rho \leq \delta$, the solution to our systems (10)-(14) is bounded for all $t > 0$, but later we can prove the boundedness without that assumption.

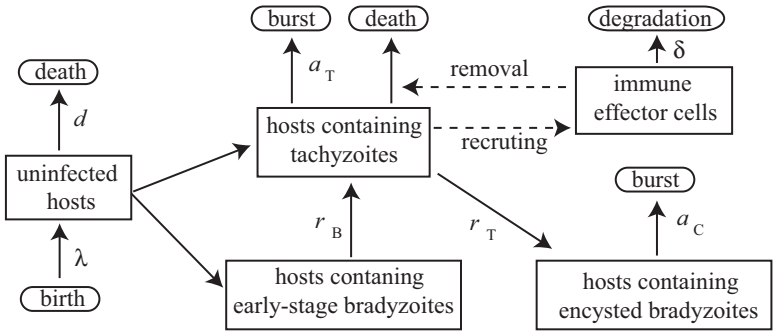

FIGURE 3. A simplified compartmental model representing the dynamics of *T. gondii*. Note the immune response is not shown.

3. **Results.**

3.1. **Disease-Free Equilibrium (DFE).**

The structure of system (10)-(14) implies there exists a unique non-negative DFE solution. Denote this equilibrium solution by

$$\mathcal{E}_0 = (X^*, Y_T^*, Y_C^*, Y_B^*, Z^*) = (X_0, 0, 0, 0, 0). \tag{15}$$

The stability of $\mathcal{E}_0$ can be established using the next generation operator method on the system (10)-(14). We take, Y_T, Y_C, Y_B, as our infected compartments, then using the notation in [39], the Jacobian matrices F and V for the new infection terms and the remaining transfer terms are respectively given by,

$$F = \begin{pmatrix} \beta_T X^* & 0 & 0 \\ 0 & 0 & 0 \\ 0 & \beta_B X^* & 0 \end{pmatrix} \text{ and } V = \begin{pmatrix} a_T + r_T & 0 & -r_B \\ -r_T & a_C & 0 \\ 0 & 0 & r_B \end{pmatrix}. \tag{16}$$

It follows that the basic reproduction number of the system (10)-(14), denoted by $\mathcal{R}_0$, is given by

$$\mathcal{R}_0 = \rho(FV^{-1}) = \frac{X_0(a_C\beta_T + r_T\beta_B)}{a_C(a_T + r_T)} \tag{17}$$

where ρ is the spectral radius. Further, using Theorem 2 in [39], the following result is established.

Lemma 3.1. *The DFE of the model (10)-(14), given by $\mathcal{E}_0$, is locally asymptotically stable (LAS) if $\mathcal{R}_0 < 1$, and unstable if $\mathcal{R}_0 > 1$.*

The basic reproduction number ($\mathcal{R}_0$) measures the average number of new infections generated by a single infected individual in a completely susceptible population [4, 11, 21, 39]. Thus, Lemma 3.1 implies that *T. gondii* can be eliminated from within the host (when $\mathcal{R}_0 < 1$) if the initial sizes of the sub-populations are in the basin of attraction of the DFE, $\mathcal{E}_0$.

Consider the domain

$$\mathcal{D}_1 = \{(X, Y_T, Y_C, Y_B, Z) \in \mathcal{D} : X^* \geq X\}.$$

Using the approach in the proof of Theorem 2.1, it can be shown that the region is positively-invariant.

Theorem 3.2. *The DFE of the model (10)-(14), given by $\mathcal{E}_0$, is global asymptotically stability (GAS) in $\mathcal{D}_1$ whenever $\mathcal{R}_0 < 1$.*

Proof. The proof is based on using a comparison theorem. The equations for the infected components in (10)-(14) can be written in terms of

$$\begin{pmatrix} \frac{dY_T(t)}{dt} \\ \frac{dY_C(t)}{dt} \\ \frac{dY_B(t)}{dt} \end{pmatrix} = \left(F - V\right) \begin{pmatrix} Y_T(t) \\ Y_C(t) \\ Y_B(t) \end{pmatrix} - MQ \begin{pmatrix} Y_T(t) \\ Y_C(t) \\ Y_B(t) \end{pmatrix} - \begin{pmatrix} 0 \\ c_T Z(t) Y_T(t) \\ 0 \end{pmatrix}, \tag{18}$$

where, $M = X^* - X(t)$, the matrices F and V are given above and Q is the non-negative matrix given by

$$Q = \begin{pmatrix} \beta_T & 0 & 0 \\ 0 & 0 & 0 \\ 0 & \beta_B & 0 \end{pmatrix}$$

Since $M \geq 0$ for all $t \geq 0$ and all parameters are positive, it follows that

$$\begin{pmatrix} \frac{dY_T(t)}{dt} \\ \frac{dY_C(t)}{dt} \\ \frac{dY_B(t)}{dt} \end{pmatrix} \leq \left(F - V\right) \begin{pmatrix} Y_T(t) \\ Y_C(t) \\ Y_B(t) \end{pmatrix}. \tag{19}$$

Using the fact that the eigenvalues of the matrix $F - V$ all have negative real parts (see the local stability result given in Lemma 3.1, where $\rho(FV^{-1}) < 1$ if $\mathcal{R}_0 < 1$ which is equivalent to $F - V$ having eigenvalues with negative real parts when $\mathcal{R}_0 < 1$ [39]), it follows that the differential inequality system (19) is stable whenever $\mathcal{R}_0 < 1$. Consequently, $(Y_T(t), Y_C(t), Y_B(t)) \to (0, 0, 0)$ as $t \to \infty$. by standard comparison results [29, 37].

The structure of the X DE gives the convergence of $X(t) \to X^*$ as $t \to \infty$. Using the convergence of $Y_T(t)$ to 0 and the term with Y_T in (14) will be smaller than the δZ term for large t, we obtain that $Z(t) \to 0$.

Thus, $(X(t), Y_T(t), Y_C(t), Y_B) \to (X^*, 0, 0, 0, 0)$ as $t \to \infty$ for $\mathcal{R}_0 < 1$. Hence, the DFE $\mathcal{E}_0$ is GAS if $\mathcal{R}_0 < 1$. □

Note that the boundedness of the solutions follows in this case.

The above result shows that *T. gondii* will be eliminated from within the host if the threshold quantity $\mathcal{R}_0$ can be brought to a value less than unity.

3.2. **Endemic Equilibrium (EE).** Let $\mathcal{E}_1 = (X^*, Y_T^*, Y_C^*, Y_B^*, Z^*)$ be any arbitrary equilibrium of the model (10)-(14). Conditions for the existence of equilibria for which *T. gondii* is endemic within the host (where at least one of the infected variables is non-zero) can be obtained as follows. Let,

$$\lambda_1^* = \beta_T Y_T^* \quad \text{and} \quad \lambda_2^* = \beta_B Y_C^*,$$

and let

$$x^* = \lambda_1^* + \lambda_2^* \tag{20}$$

be the associated force of infection, which is defined as the rate at which susceptible individuals become infected by an infectious disease [2, 14, 18, 17, 20, 34, 35]. To determine the existence of the endemic equilibrium, we consider first the case where immunity is not present (i.e $Z = 0$). Setting the right-hand sides of the model to zero gives the following expressions (in terms of λ_1^* and λ_2^* at steady state):

$$\begin{aligned} X^* &= \frac{dX_0}{(d + \lambda_1^* + \lambda_2^*)} \\ Y_T^* &= \frac{dX_0(\lambda_1^* + \lambda_2^*)}{(a_T + r_T)(d + \lambda_1^* + \lambda_2^*)} \\ Y_C^* &= \frac{dX_0 r_T(\lambda_1^* + \lambda_2^*)}{a_C(a_T + r_T)(d + \lambda_1^* + \lambda_2^*)} \\ Y_B^* &= \frac{dX_0\lambda_2^*}{r_B(d + \lambda_1^* + \lambda_2^*)}. \end{aligned} \tag{21}$$

Substituting the expression in (21) into the expression in (20) we have that the non-zero equilibrium of the model after some algebraic manipulation satisfy:

$$x^* = d(\mathcal{R}_0 - 1). \tag{22}$$

It follows that $x^* > 0$ if and only if $\mathcal{R}_0 > 1$. This result is summarized below:

Theorem 3.3. *The model (10)-(14) with $Z = 0$ has a unique endemic equilibrium whenever $\mathcal{R}_0 > 1$.*

Next we consider the case where the immune system responds throughout infection period (i.e $Z \neq 0$). To determine the existence of the endemic equilibrium, setting the right-hand sides of the model to zero gives the following expressions:

$$\begin{aligned} X^{**} &= \frac{dX_0}{(d+\lambda_1^{**}+\lambda_2^{**})} \\ Y_T^{**} &= \frac{\delta h}{(\rho-\delta)} \\ Y_C^{**} &= \frac{r_T \delta h}{a_C(\rho-\delta)} \\ Y_B^{**} &= \frac{dX_0\lambda_2^{**}}{r_B(d+\lambda_1^{**}+\lambda_2^{**})} \\ Z^{**} &= \frac{d(\lambda_1^{**}+\lambda_2^{**})(\rho-\delta)X_0 - \delta h(d+\lambda_1^{**}+\lambda_2^{**})(r_T+a_T)}{\delta h C_T(d+\lambda_1^{**}+\lambda_2^{**})}. \end{aligned} \tag{23}$$

Substituting the expression in (23) into the expression in (20) gives

$$x^{**} = \frac{\delta h(a_T+r_T)(\mathcal{R}_0-1)}{(\rho-\delta)} + \frac{\delta h(a_T+r_T)}{(\rho-\delta)} \tag{24}$$

It follows that $x^{**} > 0$ if and only if $\mathcal{R}_0 > 1$ and $\rho > \delta$. This result is summarized below:

Theorem 3.4. *The model (10)-(14) with immune response (i.e., $Z(t) > 0$) has a unique endemic equilibrium whenever $\mathcal{R}_0 > 1$ and $\rho > \delta$.*

Thus, to obtain a unique endemic equilibrium, Theorem 3.4 implies that in the presence of immune response, ρ, the maximum attack rate, must be greater than δ, the removal rate of the immune system response for this case to happen.

3.3. **Local stability of the endemic equilibrium (EE).** In this Section we will consider the stability of the endemic equilibrium $\mathcal{E}_1$. First we consider the case without immune response ($Z = 0$); thus linearizing (10)-(14) we have the matrix J evaluated at $\mathcal{E}_1$ with $Z(t) = 0$, using the equilibrium (21)

$$J = \begin{bmatrix} -d-\beta_T Y_T^* - \beta_B Y_C^* & -\beta_T X^* & -\beta_B X^* & 0 \\ \beta_T Y_T^* & \beta_T X^* - (a_T+r_T) & 0 & r_B \\ 0 & r_T & -a_C & 0 \\ \beta_B Y_C^* & 0 & \beta_B X^* & -r_B \end{bmatrix}.$$

The matrix J has the sign pattern $J_{11} < 0,\ J_{33} < 0,\ J_{44} < 0,\ J_{12}J_{21} < 0,\ J_{13}J_{31} = 0,\ J_{14}J_{41} = 0,\ J_{23}J_{32} = 0,\ J_{24}J_{42} = 0,\ J_{34}J_{43} = 0$, and $J_{22} = \frac{(a_T+r_T)(\beta_T a_C - 1)}{(a_C\beta_T + r_T\beta_B)} < 0$ provided $\beta_T a_C < 1$, thus the matrix is sign stable and hence the equilibrium (21) is locally asymptotically stable [3, 7, 22]. We have thus established the following result:

Lemma 3.5. *The endemic equilibrium (21) without immune response is locally asymptotically stable for $\beta_T a_C < 1$.*

Next we consider the stability of the equilibrium $\mathcal{E}_1$ in the presence of immune response (i.e., $Z(t) > 0$). Linearizing (10)-(14) evaluated at $\mathcal{E}_1$, using the equilibrium

(23) gives the matrix J

$$J = \begin{bmatrix} -d - Y^{**} & -\beta_T X^{**} & -\beta_B X^{**} & 0 & 0 \\ \beta_T Y_T^{**} & \beta_T X^{**} - (a_T + r_T + C_T Z^{**}) & 0 & r_B & C_T Y_T^{**} \\ 0 & r_T & -a_C & 0 & 0 \\ \beta_B Y_C^{**} & 0 & \beta_B X^{**} & -r_B & 0 \\ 0 & \frac{\rho Z^{**}}{(h+Y_T^{**})} - \frac{\rho Y_T^* Z^{**}}{(h+Y_T^{**})^2} & 0 & 0 & \frac{\rho Y_T^{**}}{(h+Y_T^{**})} - \delta \end{bmatrix}$$

where $Y^{**} = \beta_T Y_T^{**} - \beta_B Y_C^{**}$. The matrix J has the sign pattern $J_{11} < 0,\ J_{33} < 0,\ J_{44} < 0,\ J_{55} = 0,\ J_{12}J_{21} < 0,\ J_{13}J_{31} = 0,\ J_{14}J_{41} = 0,\ J_{15}J_{51} = 0,\ J_{23}J_{32} = 0,\ J_{24}J_{42} = 0,\ J_{25}J_{52} = 0,\ J_{34}J_{43} = 0,\ J_{35}J_{53} = 0,\ J_{45}J_{54} = 0,\ J_{22} = -\frac{r_T \beta_B X^{**}}{a_C} < 0$ and $J_{25}J_{52} = \frac{(\rho-\delta)(a_C\beta_T + r_T)[dX_0(\rho-\delta) - h\delta(a_T+r_T)] - a_C^2 d(\rho-\delta)^2(a_T+r_T)}{h\delta\rho(a_C\beta_T+r_T)+\rho a_C d(\rho-\delta)} < 0$ provided $dX_0(\rho-\delta) < h\delta(a_T + r_T)$, thus the matrix is sign stable and hence the equilibrium (23) is locally asymptotically stable [3, 7, 22]. We have thus established the following result:

Lemma 3.6. *The endemic equilibrium (23) with immune response is locally asymptotically stable provided* $dX_0(\rho - \delta) < h\delta(a_T + r_T)$.

4. **Discussion.** Recall from (17) that the reproduction number $\mathcal{R}_0$ is proportional to X_0, the total number of host cells before invasion of the parasites. Assuming the invasion and reproduction kinetics of the parasites are the same in different organs, larger organs intend to have more cells and thus larger $\mathcal{R}_0$ values, which will make them more suitable for the parasites to dwell. This is probably why *T. gondii* is most frequently found in brain, heart, and muscle in a host [13]. To investigate the influences of various parameters to the diseased state, we will rewrite the endemic equilibria in terms of model parameters. The equilibrium without immune response in (21) can be rewritten in terms of model parameters as follows:

$$\begin{aligned} X^* &= \frac{X_0}{\mathcal{R}_0} \\ Y_T^* &= \frac{d\,X_0}{a_T + r_T} - \frac{d\,a_C}{r_T\,\beta_B + a_C\beta_T} \\ Y_C^* &= \frac{r_T\,Y_T^*}{a_C} \\ Y_B^* &= \frac{\beta_B\,X^* Y_C^*}{r_B}. \end{aligned} \tag{25}$$

It follows from (25) that, in endemic state, the number of healthy cells, X^*, is less than the original number of cells, X_0. The model predicts that the steady state of the disease reaches a dynamic balance between three different stages of the parasites: Y_T^*, Y_C^*, and Y_B^*. Note that Y_B^* and Y_C^* are proportional to Y_T^* and Y_T^* is positively correlated to X_0. Thus, steady state parasite loads are related to the size of the organ. Also, recall the reproduction rate of uninfected cells is $\lambda = d\,X_0$. Assume the reproduction rate λ is a constant, it can be seen from (25) that, an organ with longer life expectance $1/d$ will have larger parasite loads. Since brain cells are permanent, this also explains why T. gondii is mostly like to be found in brain [13].

The equilibrium with immune response in (23) can be rewritten in terms of model parameters as follows:

$$\begin{aligned} X^{**} &= \frac{a_C\, d\, X_0(\rho-\delta)}{h\ \delta(a_C\,\beta_T+r_T\,\beta_B\,)+a_C d(\rho-\delta)} \\ Y_T^{**} &= \frac{h\,\delta}{\rho-\delta} \\ Y_C^{**} &= \frac{r_T\, Y_T^{**}}{a_C} \\ Y_B^{**} &= \frac{\beta_B\, X^{**}\, Y_C^{**}}{r_B} \\ Z^{**} &= \frac{X^{**}\,(r_T\,\beta_B + a_C\,\beta_T)-a_C(\,a_T+r_T)}{a_C\,c_T}. \end{aligned} \tag{26}$$

It is interesting to note that the relationships between the three parasite loads, Y_T^{**}, Y_C^{**}, and Y_B^{**}, remain the same as those in the absence of immune response although the steady state value of Y_T^{**} is now determined by kinetics of immune response. We also note the parasite loads Y_T^{**} and Y_C^{**} do not depend on the original number of host cells X_0 whereas the load Y_B^{**} is proportional to X_0. Moreover, when the reproduction rate of uninfected cells $\lambda = d\,X_0$ is kept at a constant, a larger life expectance $1/d$ will lead to a larger value of X^{**} and thus a higher parasite load Y_B^{**}. Again, the analysis shows that *T. gondii* favors cells with long life expectance such as the brain.

4.1. **Numerical simulations.** In order to investigate the effects of *T. gondii* infection, we first introduce model assumptions and estimate parameters of infection dynamics using experimental data available in the literature. Numerical simulations here use a mouse spleen as an example. We estimate a healthy spleen has $X_0 = 10^8$ cells. Assume that the life expectancy of spleen cells is 1 month, which leads to the death rate as $d = 1.389 \times 10^{-3}\mathrm{h}^{-1}$. In the current model, we assume at most one parasitophorous vacuole (PV) can form within a host cell. We further assume parasites within the same PV are in the same stage and replicate simultaneously. Experimental data in Weiss and Kim [40] indicate that the doubling time of tachyzoites is 6 hours and that of bradyzoites is 24 hours. Tachyzoites *in vivo* often lyse the host cell after reproducing 2 or 3 times [9]; thus, we choose $a_T = 1/(18\mathrm{h})$ and $k_T = 8/(18\mathrm{h})$. Cysts of bradyzoite may contain more than 1000 parasites [12]. We assume encysted brayzoites burst after reproducing 10 times and thus estimate $a_C = 1/(240\mathrm{h})$ and $k_C = 1024/(240\mathrm{h})$. After a parasite is released from a PV into the organ, we assume the parasite may interact with 10 host cells and the probability of invasion of individual host is 2%. It follows that $\beta_T = 8.889 \times 10^{-10}$(number of cells)$^{-1}\mathrm{h}^{-1}$ and $\beta_B = 8.533 \times 10^{-9}$(number of cells)$^{-1}\mathrm{h}^{-1}$. Since tachyzoites can convert to bradyzoites after about 20 generations of reproduction [32], we estimate $r_T = 1/\,(108\mathrm{h})$. Weiss and Kim [40] showed that 48 hours after bradyzoites invade a tissue, tachyzoites start to appear; thus, we estimate $r_B = 1/\,(48\mathrm{h})$. The current model does not consider detailed immune mechanisms. Instead, we consider the effector cells of the immune system acting on tachyzoites in PV. Assume the interaction rate between effector cells and tachyzoite PVs as $c_T = 1.67 \times 10^{-8}$(number of cells)$^{-1}\mathrm{h}^{-1}$. Assume the degradation rate of the immune effector cells to be $\delta = 1/\,(48\mathrm{h})$. Let $h = 10^5$ to account for the memory effect of immune response and let $\rho = 10/\,(24\mathrm{h})$ be the response rate.

Substituting the above parameters into Equation (17) yields $R_0 = 30.63$, which indicates that an infected cell will, on average, infect 30.63 uninfected host cells per hour. Consider an immuno-incompetent host, in which $Z = 0$, it follows that the equilibrium diseased state is $X^* = 3.26 \times 10^6$, $Y_T^* = 2.07 \times 10^6$, $Y_B^* = 6.16 \times 10^6$, and $Y_C^* = 4.61 \times 10^6$. The total number of cells is 1.61×10^7, which is reduced to 16% of the original number, X_0. In contrast, in an immunocompetent host, the long term solution is $X^* = 9.30 \times 10^7, Y_T^* = 5.26 \times 10^3$, $Y_B^* = 4.46 \times 10^5, Y_C^* = 1.17 \times 10^4$ and $Z^* = 1.07 \times 10^8$. The total number of cells is 9.34×10^7, only slightly less than the number for disease free state. Transient responses in the absence of immune response are shown in Figure 4 while transient responses in the presence of immune response are shown in Figure 5.

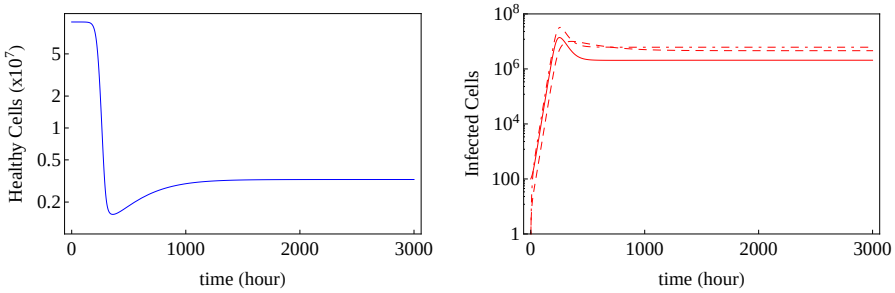

FIGURE 4. Response in the absence of immune response: variation of healthy host cells (left) and variation of infected host cells (right). The infected host cells include those infected with tachyzoites (solid), cysted bradyzoites (dashed), and early-stage bradyzoites (dotted).

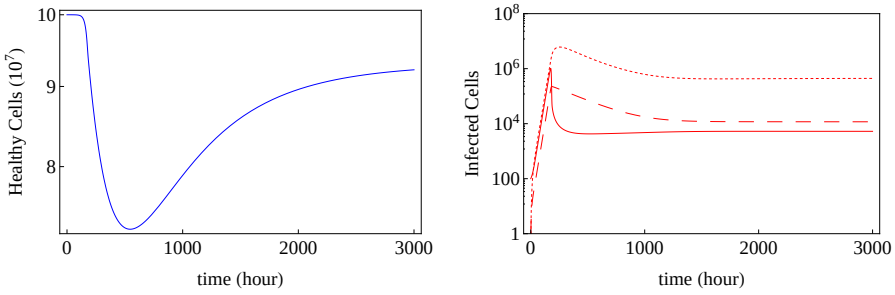

FIGURE 5. Response in the presence of immune response: variation of healthy host cells (left) and variation of infected host cells (right). The infected host cells include those infected with tachyzoites (solid), cysted bradyzoites (dashed), and early-stage bradyzoites (dotted).

We further use the model to study reactivation. While the number of parasites in an immunocompetent host is greatly suppressed, the parasites can be reactivated when the host becomes immunoincompetent [10]. Here, we consider reactivation due to temporary impairment in the immune system. We assume a host is first infected

with *T. gondii* and, after 3000 hours, the host's immune system is temporarily impaired so that the production rate ρ is reduced to 10% of the nominal value. We assume the impairment lasts for 200 hours and then the host's immunity recovers to the original level. This scenario would be analogous to a host suffering from immunodepression for a few weeks before overcoming the secondary infection and allowing for a full immune response to the toxoplasma. The results for this particular situation are shown in figure 6. It is clear that this temporary decrease in immune response leads to a significant increase of parasite load within the host.

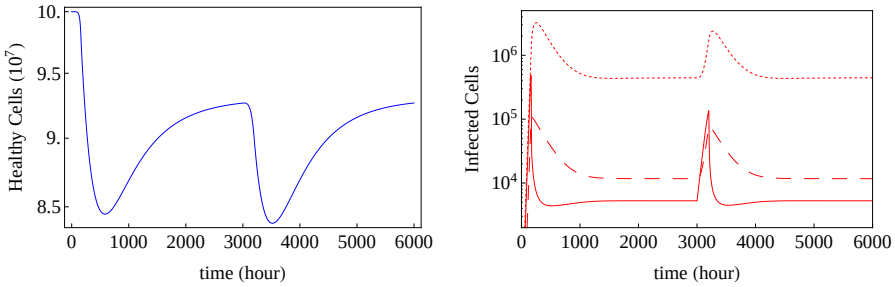

FIGURE 6. Reactivation of parasites due to temporary impairment of the immune system: variation of healthy host cells (left) and variation of infected host cells (right). The infected host cells include those infected with tachyzoites (solid), cysted bradyzoites (dashed), and early-stage bradyzoites (dotted).

5. **Conclusion.** We have developed a mathematical framework to investigate intrahost dynamics of *T. gondii*. Assumptions and simplifications have been made about the biological processes including invasion, replication, and stage conversion. Parameters of the model have been estimated based on available experimental data. In the differential equation model we created, the effects of spreading parasites are examined. In the analysis, we first found the fixed points and analyzed the rate of infection R_0. The first fixed point in the analytical model was the parasite-free equilibrium point. The second and third equilibrium points are identical in expressions for Y_T, Y_C, and Y_B. It is interesting to note that the second and third equilibrium points vary in the values for the immune response fixed point. The immune regulated equilibrium only exists when $\rho > \delta$.

It is also important to note the assumption made in analyzing this model. We have assumed the invasion dynamics of the free parasites are much faster than the replication and stage conversion, which leads to quasistationary simplification of the free parasites. This assumption is valid because the bursting of cells with tachyzoites release free tachyzoites, this release was modeled as a contribution of infection directly to uninfected hosts. The use of the Holling's Type II functional response models the way an immune system should respond: Very limited response to low numbers of invaders and a quickly growing response up to a threshold as the number of invaders increases. This type of response allows us to simplify the immune system into a mathematical model.

The critical value for R_0 found in this model indicates that our infection rate is dependent upon the initial number of uninfected hosts, the death rate of cells infected with bradyzoites and tachyzoites, the invasion rate of tachyzoites and bradyzoites

contained within a host, and the conversion rate from tachyzoites to bradyzoites. Analyses of the reproduction number and the endemic solutions indicate that *T. gondii* favors large organs with long life expectance. This agrees with the experimental observation that T. gondii are commonly found in skeletal muscles, brain, and myocardium.

Numerical simulations show that the immune system plays a pivotal role in suppressing the growth of tachyzoites within host cells. This suppression, once the system reaches endemic behavior, allows for the body to exit the acute infection stage and begin the long-term, virtually symptom-free, state. Without immune response, the tachyzoites would be free to replicate and invade many different hosts.

Tachyzoites are rapidly dividing and responsible for the acute infection whereas the slowly replicating bradyzoites are located within tissue cysts, which protect the parasite from the host immune system and make it inaccessible to drugs [13]. The differentiation of tachyzoites into bradyzoites is a response to the onset of protective immunity whereas the dormant bradyzoites are able to reconvert into tachyzoites to cause fatal infection in patients. Therefore, stage conversion between tachyzoites and bradyzoites plays a pivotal role in the pathogenesis, transmission, persistence, and reactivation of the disease.

Future work of this system will include a more detailed description of immune response. While using the Holling's Type may accurately model the conceptual framework of an immune response, more evidence is needed to qualify this technique as accurate. A further expansion of this model might include a spatial array in which the disease can propagate. While our model tracks the disease throughout the spleen and assumes a homogenous distribution of cells throughout, the parasites are actually capable of starting in the stomach and invading the brain, muscles, and liver. Therefore, a spatial model may be able to describe the complicated dynamics that describe how the parasites can move throughout the body.

Acknowledgments. This work was assisted through participation in the Modeling Toxoplasma *gondii* Investigative Workshop and the Multiscale Modeling of the Life Cycle of Toxoplasma *gondii* Working Group at the National Institute for Mathematical and Biological Synthesis (NIMBioS), sponsored by the National Science Foundation, the U.S. Department of Homeland Security, and the U.S. Department of Agriculture through NSF Award #EF-0832858, with additional support from The University of Tennessee, Knoxville. Agusto and Bewick are Postdoctoral Fellows at NIMBioS. This work was in part supported by NSF under grant No. CMMI-0845753. The authors would like to thank Yasuhiro Suzuki, Vitaly Ganusov, Matthew Turner, Don Hinton, and Michael Gilchrist for their insightful discussions.

REFERENCES

[1] Centers for Disease Control and Prevention, *Toxoplasmosis*, November 2010. Available from: http://www.cdc.gov/toxoplasmosis/.

[2] F. B. Agusto and A. B. Gumel, *Theoretical assessment of avian influenza vaccine,* DCDS Series B, **13** (2010), 1–25.

[3] F. B. Agusto and O. R. Ogunye, *Avian Influenza optimal seasonal vaccination strategy,* ANZIAM Journal, **51** (2010), 394–405.

[4] R. M. Anderson and R. May, "Infectious Diseases of Humans," Oxford University Press, New York, 1991.

[5] A. J. Arenas, G. Gonzalez-Parra and R. V. Mico, *Modeling toxoplasmosis spread in cat populations under vaccination,* Theoretical Population Biology, **77** (2010), 227–237.

[6] F. Brauer and C. Castillo-Chávez, "Mathematical Models in Population Biology and Epidemiology," Texts in Applied Mathematics, **40**, Springer, New York, 2001.
[7] F. Brauer and P. van den Driessche, *Models for transmission of disease with immigration of infectives*, Math. Biosc., **171** (2001), 143–154.
[8] L. Chen, F. Chen and L. Chen, *Analysis of a predator-prey model with holling type II functional response incorporating a constant prey refuge,* Nonlinear Analysis: Real World Applications, **11** (2010), 246–252.
[9] M. da Fonseca, F. da Silva, A. C. Takács, H. S. Barbosa, U. Gross and C. G Lüder, *Primary skeletal muscle cells trigger spontaneous toxoplasma gondiitachyzoite-to-bradyzoite conversion at higher rates than fibroblasts,* International Journal of Medical Microbiology, **299** (2009), 381–388.
[10] R. C. da Silva, A. V. da Silva and H. Langoni, *Recrudescence of Toxoplasma gondii infection in chronically infectedrats (Rattus norvegicus)*, Experimental Parasitology, **125** (2010), 409–412.
[11] O. Diekmann, J. A. P. Heesterbeek and J. A. J. Metz, *On the definition and computation of the basic reproduction ratio R_0 in models for infectious diseases in heterogeneous populations,* J. Math. Biol., **28** (1990), 365–382.
[12] J. P. Dubey, D. S. Lindsay and C. A. Speer, *Structures of toxoplasma gondii tachyzoites, bradyzoites, andsporozoites and biology and development of tissue cysts,* Clin. Microbiol. Rev., **11** (1998), 267–299.
[13] J. P. Dubey, "Toxoplasmosis of Animals and Humans," CRC Press, 2010.
[14] L. Esteva, A. B. Gumel and C. V. de León, *Qualitative study of transmission dynamics of drug-resistant malaria,* J. Mathematical and Computer Modelling, **50** (2009), 611–630.
[15] D. J. Ferguson, *Toxoplasma gondii andsex: Essential or optional extra?*, Trends Parasitol., **18** (2002), 355–359.
[16] D. Filisetti and E. Candolfi, *Immuneresponse to toxoplasma gondii,* Ann Ist Super Sanita, **40** (2004), 71–80.
[17] S. M. Garba and A. B. Gumel, *Effects of cross-immunity on the transmission dynamics of two strains of dengue,* International Journal of Computer Mathematics, **87** (2010), 2361–2384.
[18] S. M. Garba, A. B. Gumel and M. R. Abu Bakar, *Backward bifurcations in dengue transmission dynamics,* Mathematical Biosciences, **215** (2008), 11–25.
[19] G. C. Gonzalez-Parra, A. J. Arenas, D. F. Aranda, R. J. Villanueva, L. Jódar, *Dynamics of a model of Toxoplasmosis disease in human and cat populations,* Computers and Mathematics with Applications, **57** (2009), 1692–1700.
[20] A. B. Gumel, *Global dynamics of atwo-strain avian influenza model,* International Journal of Computer Mathematics, **86** (2009), 85–108.
[21] H. W. Hethcote, *The mathematics of infectious diseases,* SIAM Rev., **42** (2000), 599–653.
[22] C. Jeffries, V. Klee And P. van den Driessche, *When is a matrix sign stable?,* Can. J. Math., (1977) **29**, 315–326.
[23] M. E. Jerome, J. R. Radke, W. Bohne, D. S. Roos and M. W. White, *Toxoplasma gondii bradyzoites form spontaneously during sporozoite-initiated development,* Infection and Immunity, **66** (1998), 4838–4844.
[24] W. Jiang, A. Sullivan, C. Su and X. Zhao, *An agent-based model for the transmission dynamics of toxoplasma gondii,* Journal of Theoretical Biology, **293** (2012), 15–26.
[25] M. Lélu, M. Langlais, M.-L. Poulle and E. Gilot-Fromont, *Transmission dynamics of toxoplasma gondii along an urban-rural gradient*, Theoretical Population Biology, (2010), 139–147.
[26] B. Kafsack, V. B. Carruthers and F. J. Pineda, *Kinetic modeling of toxoplasma gondii invasion,* Journal of Theoretical Biology, **249** (2007), 817–825.
[27] M. J. Keeling and P. Rohani, "Modeling Infectious Diseases in Humans and Animals," Princeton University Press, Princeton, NJ, 2008.
[28] M. Kot, "Elements of Mathematical Ecology," Cambridge University Press, 2003.
[29] S. Leela, V. Lakshmikantham and A. A. Martynyuk, "Stability Analysis of Nonlinear Systems," Monographs and Textbooks in Pure and Applied Mathematics, **125**, Marcel Dekker, Inc., New York, 1989.
[30] J. D. Murray, "Mathematical Biology. I. An Introduction," Third edition, Interdisciplinary Applied Mathematics, **17**, Springer-Verlag, New York, 2002.
[31] M. A. Nowak and R. May, "Virus Dynamics: Mathematical Principles of Immunology and Virology," Oxford University Press, Oxford, 2000.

[32] J. R. Radke, R. G. Donald, A. Eibs, M. E. Jerome, M. S. Behnke, P. Liberator and W. W. White, *Changes in the expression of the human cell division autoantigen-1 influence toxoplasma gondii growth and development,* PLoS Pathog., **2** (2006), 105.
[33] Z. Qiu, J. Yu and Y. Zou, *The asymptotic behaviour of a chemostat model*, Discr. Cont. Dynam. Syst. Ser. B, **4** (2004), 721–727.
[34] O. Sharomi, C. N. Podder, A. B. Gumel and B. Song, *Mathematical analysis of the transmission dynamics of HIV/TB co-infection in the presence of treatment,* Mathematical Biosciences and Engineering, **5** (2008), 145–174.
[35] O. Sharomi and A. B. Gumel, *Re-infection-induced backward bifurcation in the transmission dynamics of Chlamydia trachomatis,* Journal of Mathematical Analysis and Applications, **356** (2009), 96–18.
[36] G. Skalski and J. Gilliam, *Functional responses with predator interference: Viable alternatives to the holling type II model,* Ecology, **82** (2001), 3083–3092.
[37] H. L. Smith and P. Waltman, "The Theory of the Chemostat. Dynamics of Microbial Competition," Cambridge Studies in Mathematical Biology, **13**, Cambridge University Press, Cambridge, 1995.
[38] M. Turner, S. Lenhart, B. Rosenthal, A. Sullivan and X. Zhao, *Modeling effective transmission strategies and control of the world's most successful parasite,* submitted.
[39] P. van den Driessche and J. Watmough, *Reproduction numbers and sub-threshold endemic equilibria for compartmental models of disease transmission,* Math. Biosci., **180** (2002), 29–48.
[40] L. Weiss and K. Kim, "Toxoplasma Gondii," Academic Press, 2007.
[41] D. Wodnarz, "Killer Cell Dynamics. Mathematical and Computational Approaches to Immunology," Springer-Verlag, New York, 2007.

Received July 29, 2011; Accepted May 14, 2012.

E-mail address: asulli17@utk.edu
E-mail address: fbagusto@gmail.com
E-mail address: sharon.bewick@gmail.com
E-mail address: csu1@utk.edu
E-mail address: lenhart@math.utk.edu
E-mail address: xzhao9@utk.edu